The Mid-Pleistocene and the Pliocene-Pleistocene transitions, clues of the resonance of the climate system in subharmonic modes

J-L Pinault[1]

[1]Independent scholar, 96, rue du Port David, 45370 Dry, France

Corresponding author: Jean-Louis Pinault (jeanlouis_pinault@hotmail.fr)

Key Points:

- A transition similar to that of the Mid-Pleistocene occurred at the hinge of Pliocene-Pleistocene, involving 10 times longer periods
- The climate system preferentially responds to certain orbital variations according to subharmonic modes

Abstract

How variations in Earth's orbit pace the glacial-interglacial cycles of the Quaternary are probably one of the greatest mysteries of modern climate science. Supposing coevolution of climate, ice sheets, and carbon cycle over the past 3 million years a current theory cannot explain the observations when it is driven by orbital variations as the only external forcing. Taking advantage of the alkenone paleothermometer in sediment cores sampled in the Tasman Sea floor, we show that the transition of glacial-interglacial periods from 41,000- to 100,000-year that happened during the mid-Pleistocene is not singular. A similar transition involving 10 times longer periods occurred at the hinge of Pliocene-Pleistocene. Referring to the recent theory of gyral Rossby waves we put forward the idea that the climate system preferentially responds to certain orbital variations according to subharmonic modes, which is inherited from the resonant forcing of Rossby waves wrapping around the subtropical gyres.

1 Introduction

1.1 Motivation

While most climate transitions have been recognized as resulting from solar and orbital forcing due to their synchronism, understanding the underlying physical mechanisms is encountering considerable problems. Probably the most important of these reflects the lack of proportionality between the alleged cause and the effect. Difficulties reach their culmination when the Mid-Pleistocene Transition (MPT) is considered, that is a fundamental change in the behavior of glacial cycles during the Quaternary glaciations. The transition happened approximately 1.2 million years ago, in the Pleistocene epoch. Before the MPT, the glacial cycles were dominated by a 41,000-year periodicity coherent with the Milankovitch forcing from axial tilt. After the MPT the cycle lengths have increased, with an average length of approximately 100,000 years coherent with the Milankovitch forcing from eccentricity. However, the intensity of the forcing resulting from the eccentricity is much lower than that induced by the axial tilt.

Solar and orbital forcing of the climate system suggests that resonances occur, the forcing efficiency strongly depending on the periods. This has led some researchers to propose different mechanisms that can produce resonances. Stochastic resonance has been investigated, suggesting slow changes of climate are the integral response to continuous random excitation by short period disturbances (Hasselmann, 1976, Benzi et al., 1982, Nicolis, 1982, Matteucci, 1991). This concept has been applied to large-scale, long-time sea surface temperature (SST) anomalies as the response of the oceanic surface layers to short-time-scale atmospheric forcing (Frankignoul and Hasselmann, 1977, Saravanan and McWilliams, 1997). The role of stochastic freshwater forcing on the generation of millennial-scale climate variability in the North Atlantic has been studied using a coupled atmosphere–ocean–sea ice model (Ya, 1980, Ganopolski and Rahmstorf, 2002, Timmermann et al., 2003). These models are based on general principles and are more intended to propose amplification mechanisms than to explain precisely what is observed from climate records.

More precise models have been proposed to explain the MPT, involving long-term changes in atmospheric CO2 over the Quaternary (Clark et al., 2006, Chalk et al., 2017). A recent paper supposes the coevolution of climate, ice sheets, and carbon cycle over the past 3 million years (Brovkin et al., 20190). It suffers from an arbitrary condition that is the precise timing of the transition depending on the optimal regolith removal scenario prescribed additionally to orbital forcing. In addition, like all models involving ice sheets, it assigns a special role to the northern hemisphere glaciation while climate records show that the glacial-interglacial cycles are planetary phenomena. Without being able to justify the resonant nature of the climate system, this model cannot reproduce the observations when it is driven by orbital variations as the only external forcing.

Referring to the recent theory of Gyral Rossby Waves (GRWs) the climate system preferentially responds to certain orbital variations, which is inherited from the resonant forcing of Rossby waves wrapping around the subtropical gyres (Pinault, 2018a, b, c, 2020a). Formed where the boundary currents leave the continents to re-enter the subtropical gyres, several approximately non-dispersive long-period Rossby waves overlap. This new concept that is the subject of this paper not only explains the considerable variations in the efficiency of forcing over time as occurs during the MPT, but also the transformations of the gyres observed when they adjust to the different conditions of forcing to tune their natural periods to the forcing periods.

1.2 Related work

Contrary to the concepts exposed previously, that proposed here leads to constrained results, which reinforces its likelihood because having only an extremely low number of degrees of freedom. Applied to the modulated currents of the subtropical gyres, the equations of motion of coupled oscillators with inertia, whose prototypes are the Caldirola–Kanai oscillators, require that the periods of GRWs are subharmonics of annual Rossby waves. Subharmonic modes ensure the durability of the resonant dissipative system, with each oscillator transferring as much interaction energy to all the others that it receives periodically (Pinault, 2018a).

Subharmonic modes are determined experimentally from the observed periods of GRWs. From periods extending from 64 years (n_1=2^0) to 98.3 Ka (n_{11}=3×2^9) they were deduced both from direct observation of Rossby waves along the ocean gyres, but also from climate records. Indeed, the oscillation of the thermocline impacts the climate system by stimulating or, on the contrary, by reducing the heat exchanges between the surface of the gyres and the atmosphere. The main modes are 768 years ($n_4 = 3 \times 2^2$) that may trigger little ice ages during the Holocene, 24,576 ($n_9 = 3 \times 2^7$), 49,152 ($n_{10} = 3 \times 2^8$), and 98,304 ($n_{11} = 3 \times 2^9$). that contribute to glacial-interglacial cycles.

The aim of this article is to extend the list of subharmonic modes whose periods are greater than 98.3 Ka while specifying the resonant nature of GRWs and their climatic effects.

2 Materials and Methods

2.1 Sea Surface Temperatures at DSDP Site 593

Sea Surface Temperatures at DSDP Site 593 presently situated north of the subtropical front, in the Tasman Sea, allows to extend subharmonic modes beyond what was explored previously due to the high resolution of the climate archive which spans 3.5 million years. Location of the DSDP Site 593 is favorable for the observation of the seawater temperature of the South Pacific gyre in its most southern part. It is indeed interpreted as evidence for varying influences of subtropical (warm) and sub-Antarctic (cold) waters in the southern Tasman Sea. The optimal conditions are met for the study of the South Pacific gyre from observation of the subtropical front over time.

Given the time scales, measurement of the sea surface temperature using the alkenone paleothermometer (McClymont et al., 2016) in sediments (diagenetic product of chlorophyll) is not only representative of the sea surface temperature (SST) but also of deeper waters. The main interest of this proxy is its sensitivity to temperature variations. Furthermore, it does not suffer from remanence phenomena as is the case for dissolved species due to exchanges with different reservoirs during diagenetic processes, which is detrimental to the time resolution.

2.2 Temperatures at DSDP Site 593 compared to EPICA data

Comparison of the SST at DSDP Site 593 calibrated from alkenone concentration in sediment cores and EPICA temperature calibrated from Deuterium concentration in ice cores, both filtered in the band 73.7, 147.5 Ka, shows that the SST data are 1.25 lower than the EPICA data. Comparison is carried out over 280 Ka BP, that is the time interval for which the time resolution of both series allows it.

3 Data

Data referring to orbital variations calculated by Berger and Loutre (1991) are available at: https://www1.ncdc.noaa.gov/pub/data/paleo/climate_forcing/orbital_variations/insolation/orbit91

Alkenone and benthic foraminiferal Mg/Ca paleothermometers at Deep Sea Drilling Project (DSDP) Site 593 in the Tasman Sea, southwest Pacific are available vs time (McClymont et al., 2016) at: https://www1.ncdc.noaa.gov/pub/data/paleo/contributions_by_author/mcclymont2016/mcclymont2016-dsdp593.txt

4 Results and discussion

4.1 The Pacific subtropical gyre during the MPT

Why the insolation variations and their effects observed on the temperature of sea water at high latitudes of the gyres are not proportional stems from the dependence of the efficiency of resonant forcing of GRWs in subharmonic modes, and the deviation between the forcing and natural periods (Pinault, 2020a). But the relevance of GRWs is not only worthy of interest in the analysis of the causes of the MPT, but also for explaining the observed modifications of the circumference of the subtropical gyres following this event whose impact is considerable. For this, the Tasman Sea is rich in observations, being subject to both the warm subtropical front and the cold sub-Antarctic front of the Antarctic Circumpolar Current. The history of currents over the last million years is traced thanks to the sediment cores sampled from the ocean floor through ocean deep drilling programs.

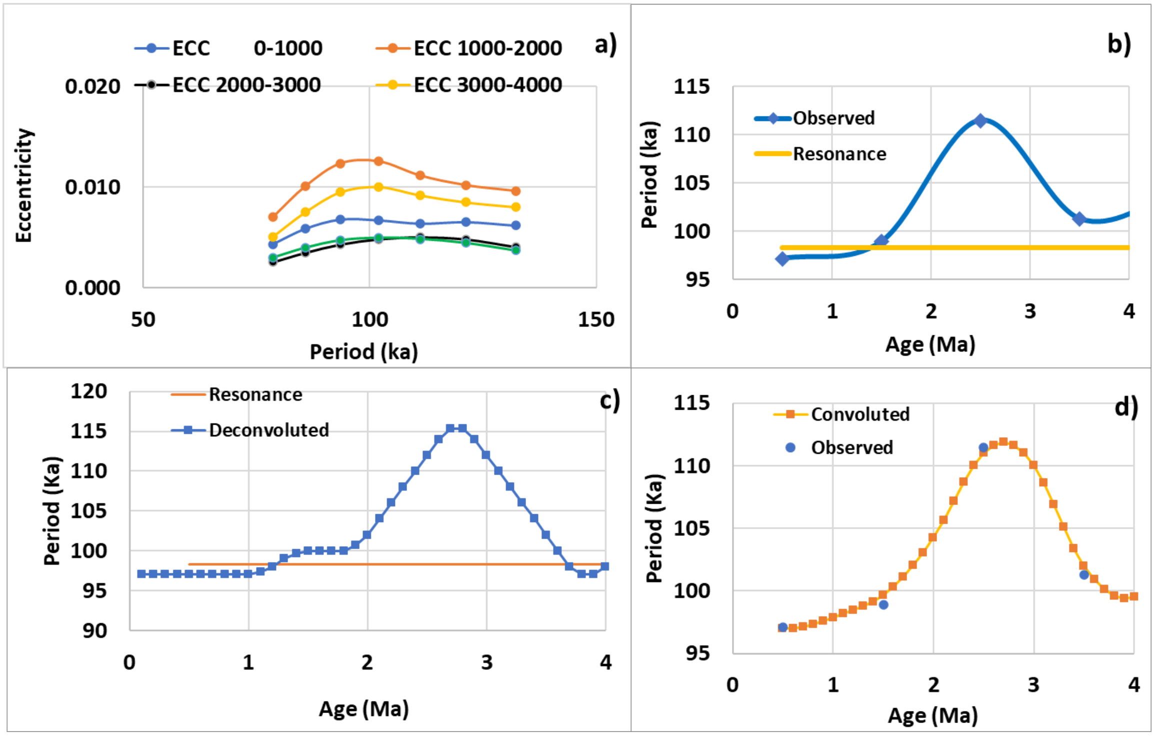

Fig. 1 – Variations in the period of eccentricity in the vicinity of 100 Ka - a) Fourier transform of eccentricity variations over 1 Ma time intervals – b) Periods vs time observed at the maximums of the Fourier transforms in a) – c) Deconvoluted curve of the period vs time represented in b) – d) Comparison of the moving average over 1 Ma of the deconvoluted curve in c) and the period vs time in b).

The evolution of the period of eccentricity over a few million years BP is deduced from the orbital calculations (Berger and Loutre, 1991). Because it is subject to a large variability, the Fourier spectra are averaged over 1 Ma (Fig. 1a), which results from a compromise between time and frequency resolution. Despite this time averaging, the Fourier transform has a spread maximum which is not conducive to determining the orbital forcing frequency with precision. The Fourier spectrum being approached by a parabola near its maximum, this is calculated analytically.

On the other hand, the integration over intervals of 1 Ma of the period requires that its representation as a function of time is deconvoluted. A solution is shown in Fig. 1c, the one that is as smooth as possible to be the more realistic. Performing a moving average over 1 Ma of the solution allows faithfully reconstructing the initial period vs time (Fig. 1d).

According to Fig. 1c the period of eccentricity varies greatly over the last 4 million years, approaching the period of resonance of the subharmonic mode n_{11}, namely 98.3 Ka, since 1.2 Ma BP. A natural period of the GRWs becoming close to the forcing period, the gyres adjust to perfect the tuning between both periods. While the dominant period of the glacial-interglacial cycles before the MPT was 41 Ka, coherent with the obliquity, it has since been coherent with that of eccentricity although the amplitude of the orbital forcing is much higher for the obliquity than for the eccentricity.

The assumption that the GRWs were tuned to different forcing periods before and after the MPT assumes that the dominant period was 41 Ka before the MPT, as attested by the climate records. However, the closest natural period corresponds to the subharmonic mode n_{10}, namely 49.2 ka. The transition of the period from 41 Ka, when the subharmonic mode n_{10} was tuned to the forcing period before the MPT, to the natural period of 49.2 Ka at present requires an adjustment of the gyre.

As the dispersion relation shows (Pinault, 2018b), lengthening of the period requires either an equatorward shift of the centroid of the gyre or an increase in its circumference. In the first case, the latitudinal displacement of the centroid increases the cyclonic phase velocity for an observer dragged along the wind-driven circulation but reduces the apparent anticyclonic phase velocity for a fix observer. In the second case, increasing the circumference lengthens the period since the phase velocity remains unchanged.

Considering together paleothermometers at DSDP Site 593 and ODP 1172, it is inferred that, during late Pliocene, a poleward displacement of the subtropical front compared to modern occurred between 40 and 44°S (McClymont et al., 2016). Obviously the second hypothesis is the correct one. A 4 ° drift of the subtropical front towards the south without displacement of the centroid of the gyre increases the circumference by almost 20%, which reflects the adjustment of the gyre to move the natural period of the subharmonic mode n_{10} from 41 to 49.2 Ka. In this way, the drift of the subtropical front concomitantly with the MPT confirms the hypothesis that the latter results from bringing closer the natural period of the subharmonic mode n_{11}, namely 98.3 Ka and the forcing period resulting from the eccentricity variations.

4.2 Subharmonic modes

When used as a proxy of SST (Fig. 2a), alkenone concentration in sediment cores at DSDP Site 593 allows to accurately extend the properties of four subharmonic modes from n_{12} to n_{15}. As shown in Fig. 2b the Fourier transform (FT) of SST vs time highlights the periods of the main oscillations, that is, 218, 476, and 1131 Ka. However, the analysis of the coherency () between the variations in the total solar irradiance (TSI) resulting from orbital forcing obliterates the peak at 218 Ka, only two peaks, one at 440 Ka and the other at 1046 Ka are visible (Fig. 2e), which suggests an effective orbital forcing in this case.

It turns out that the first peak of the FT of SST is close to the period relative to the subharmonic mode $n_{12} = (3 \times 2^9) \times 2 = 3 \times 2^{10}$=3072 whose period is 3072×64 =196.6 Ka (the subharmonic mode is expressed using the Atlantic Ocean as a reference). Since this peak does not appear in the coherence spectrum, the GRW must be considered as a pure harmonics of longer period GRWs. Note that the coherence spectrum (Torrence and Compo, 1998) between two series varies from 0 to 1, the maximum value being reached between two sinusoids of the same period, in a bandwidth of infinite width.

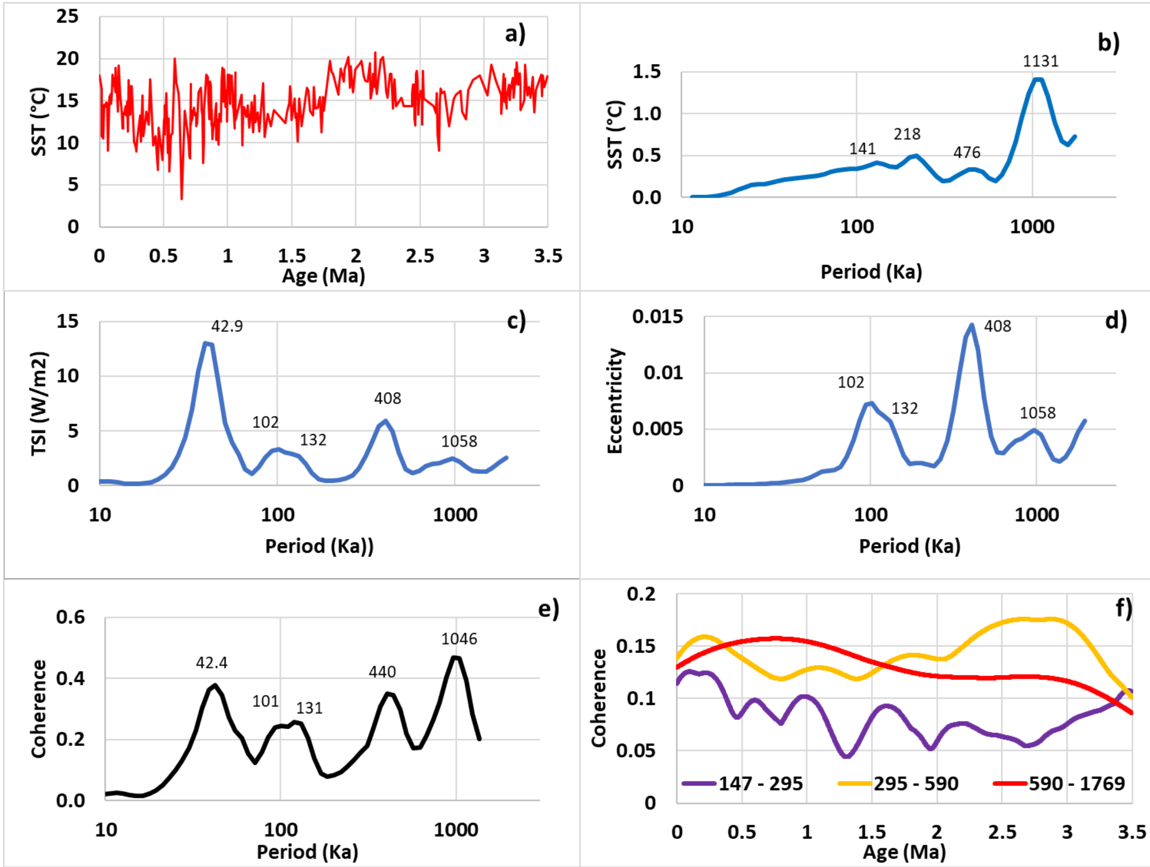

Fig. 2 - Data used in the present study - a) Alkenone concentration vs time at DSDP Site 593 used as a proxy of Sea Surface Temperatures (SST) – b) Fourier transform (FT) of SST vs time. Maximums of the peaks are in Ka – c) FT of Total Solar Irradiance (TSI) - d) FT of eccentricity variations - e) Coherence of TSI and SST vs period – f) Coherence of TSI and SST vs time

In the coherence spectrum, the two peaks highlight the forcing from variations in eccentricity, the only orbital parameter whose period exceeds 41 Ka (Fig. 2d). The first refers to the subharmonic mode $n_{13} = (3 \times 2^{10}) \times 2 = 3 \times 2^{11}$=6144 whose period is 6144 ×64 =393.2 Ka. It appears that the mode for which the period is closest to the second peak is $n_{14} = (3 \times 2^{11}) \times 3 = 3^2 \times 2^{11}$=18,432 whose period is 18432×64 =1,180 Ka.

4.3 The band 295-590 Ka

Table 1 - The natural periods of Gyral Rossby Waves (GRWs), and the bands characteristic of subharmonic modes. Subharmonic modes in the North and South Pacific must be divided by 2 and multiplied by 3/2 in the South Indian Ocean. Subharmonic modes in bold are the subject of this present work.

Rank	Band Width (yr)	Period of Resonance (yr)	Subharmonic Mode in the Atlantic	Forcing Mode
12	**147456-294912**	**196608**	$\mathbf{3 \times 2^{10}}$	**No external forcing**

13	**294912-589824**	**393216**	3×2^{11}	**Orbital forcing (eccentricity)**
14	**589824-1769472**	**1179648**	$3^2 \times 2^{11}$	**Orbital forcing (eccentricity)**
15	**1769472-3538944**	**2359296**	$3^2 \times 2^{12}$	**No external forcing**

Comparison of TSI and de-trended SST filtered into the band 295-590 Ka characteristic of the subharmonic mode n_{13} (Table 1, Fig. 3) confirms that they are coherent because they are nearly in phase, a prerequisite for supporting a causal relationship between forcing and its effects on subtropical ocean gyres (Pinault, 2018b). However, the forcing efficiency varies over time since the oscillation of the SST weakens between 1.6 and 2.4 Ma BP while the forcing remains sustained throughout the duration of the observation. Indeed, Fig. 3b confirms the weakening of the forcing efficiency despite the vicinity of forcing and natural periods, that is, 408 and 393.2 Ka.

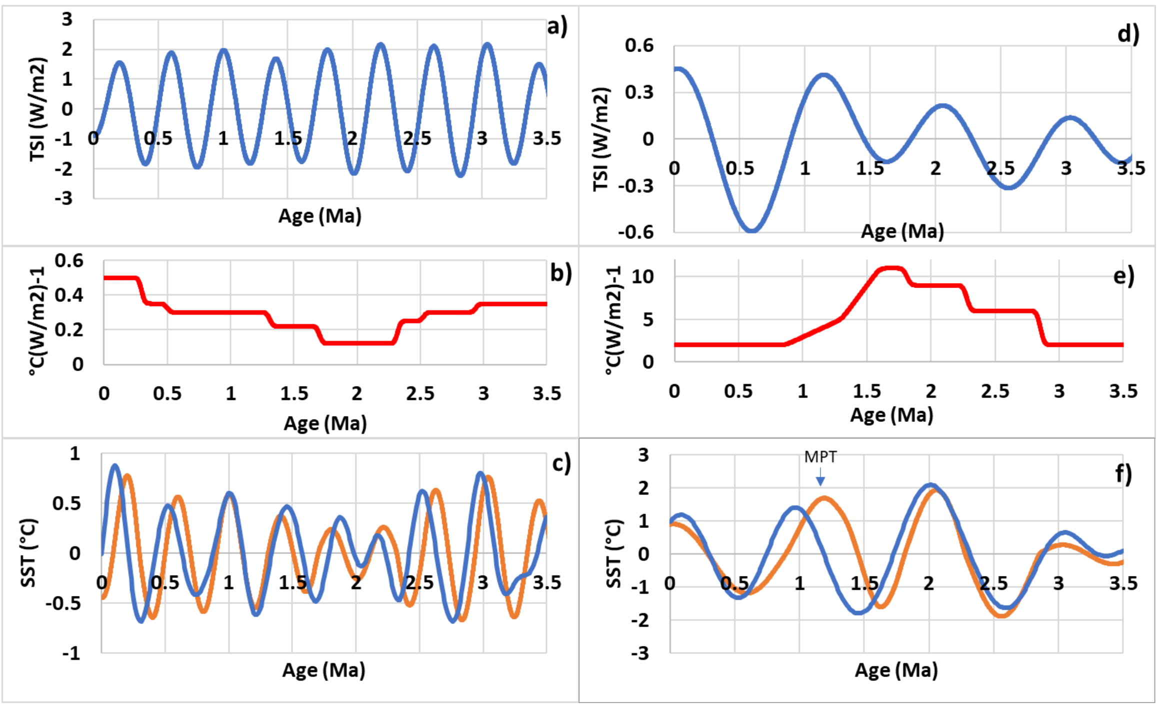

Fig. 3 – Orbital forcing and SST response into the band 295-590 Ka – a) Total solar irradiance (TSI) – b) Forcing efficiency – c) Comparison of the TSI multiplied by the forcing efficiency from (b) and the SST - d), e), f) same as a), b), c) transposed to the band 590-1769 Ka.

4.4 The band 590-1769 Ka

As in the band 295-590 Ka, comparison of TSI and de-trended SST filtered into the band 590-1769 Ka characteristic of the subharmonic mode n_{14} shows that they are nearly coherent, apart from the slight phase shift which occurred between 1.5 and 0.8 Ma BP, which might reflect the adjustment of the gyre during the MPT (Fig. 3f). As shown in Fig. 3e the forcing efficiency increases considerably during the transition Pliocene-Pleistocene, overreaching 10 °C (W / m^2)$^{-1}$. Such a value denotes an optimum tuning between the natural and the forcing periods. The mode n_{13} is multiplied by 3 to obtain the mode n_{14} instead of 2: this reflects the strong influence of the forcing resulting from the eccentricity variations.

4.5 The band 1769-3539 Ka

Due to the limitation imposed by the duration of the observations, the investigated bandwidth is 1769-3500 Ka, which does not enable the FT of the series. SST filtered into this band (Fig. 4b) exhibits an oscillation whose period is estimated nearly 2.27 Ma (half-period between 0.877 and 2.01 Ma). This period corresponds to the subharmonic mode $n_{15} = (3^2 \times 2^{11}) \times 2 = 3^2 \times 2^{12}$=36,864 whose natural period is 36864×64 =2,359 Ka. This time, it is probably a pure subharmonic because de-trended SST and TSI filtered into this band are out of phase (Fig. 4a, b).

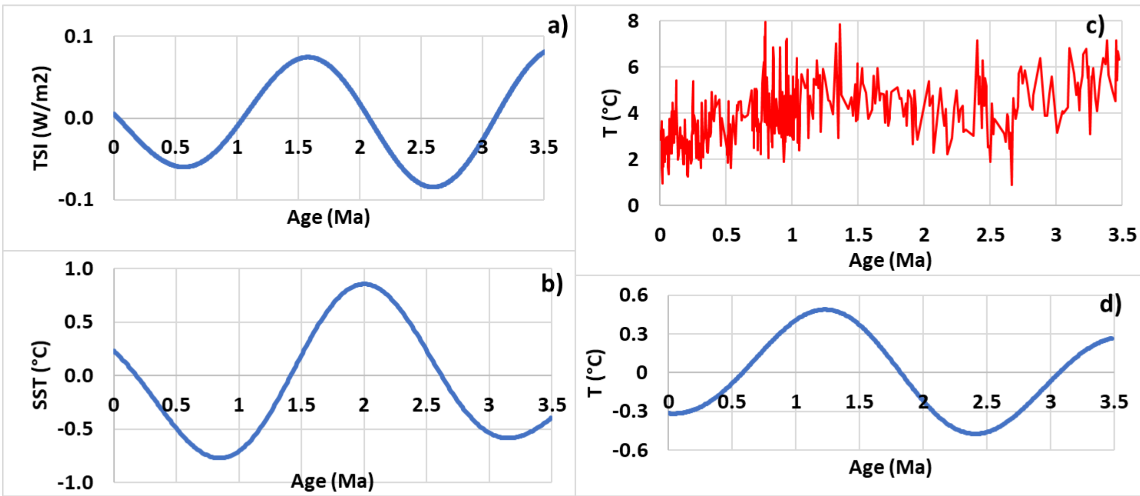

Fig. 4 – Orbital forcing and responses of SST and sea water temperature (T) into the band 1769-3500 Ka – a) Total Solar Irradiance (TSI) - b) SST de-trended and filtered – c) Benthic foraminiferal Mg/Ca analysis vs time at DSDP Site 593 used as a proxy of T – d) T de-trended and filtered

Benthic foraminiferal Mg/Ca analysis at DSDP Site 593 is another paleothermometer: given the residence times of Mg (~14 Ma) and Ca (~1 Ma), the ocean temperature reconstructions from the Mg/Ca ratio is subject to a low band-pass filter (Fig. 4c, d) so that the 1.08 Ma period oscillation disappears to the benefit of the longer period oscillation that refers to the subharmonic mode n_{15}. It not only has the effect of filtering the high frequencies but also of delaying the phase of the oscillation by about 0.7 Ma while attenuating its amplitude. However, this allows the accurate estimation of the half-period between 1.24 Ma and 2.43 Ma, which estimates the period close to 2.38 Ma even more convincingly because here only one oscillation is isolated.

4.6 The Pliocene-Pleistocene transition

A resonance phenomenon comparable to what is observed during the MPT occurs at the hinge of the Pliocene and the Pleistocene. This is illustrated by the Fig. 5, the only difference with the Fig. 1 being that, here, the periods are 10 times higher than previously, which requires the FT is performed on successive intervals of time of 2500 Ka instead of 1000 Ka (Fig. 5a). Time intervals overlap to represent the period vs time.

Whether it is Mid-Pleistocene or Pliocene-Pleistocene transition, two subharmonic modes are forced simultaneously. They are n_{10} and n_{11} whose natural periods are 49.2 and 98.3 Ka during the first transition, and n_{13} and n_{14} whose natural periods are 0.39 and 1.18 Ma during the second. The natural period of the highest mode tunes transiently, but optimally, to the forcing period when both become very close (Fig. 1c, Fig. 5c). Then, the two subharmonic modes swap the dominant mode. as attested by the nearly symmetrical opposite variation in the forcing efficiencies (Fig. 3b, e). The forcing efficiency of the higher mode exceeds 10 °C (W / m^2) $^{-1}$ between 2.4 and 1.6 Ma BP when the tuning is optimal whereas that of the lower mode drops to 0.12 °C (W / m^2) $^{-1}$. The change in the dominant period occurred approximately 2.5 Ma ago when the 0.39 Ma period oscillation collapsed in favor of the 1.18 Ma period oscillation (Fig. 3c, f). Nowadays the transition is occurring in the other direction since the 1.18 Ma period oscillation is collapsing in favor of the 0.39 Ma period oscillation, both having approximately the same amplitude. This transition involves a weak adjustment in the circumference of the gyre because the deviation between the forcing and natural periods of the lower subharmonic mode is small, 0.41 and 0.39 Ma respectively (Table 1, Fig. 2c, d).

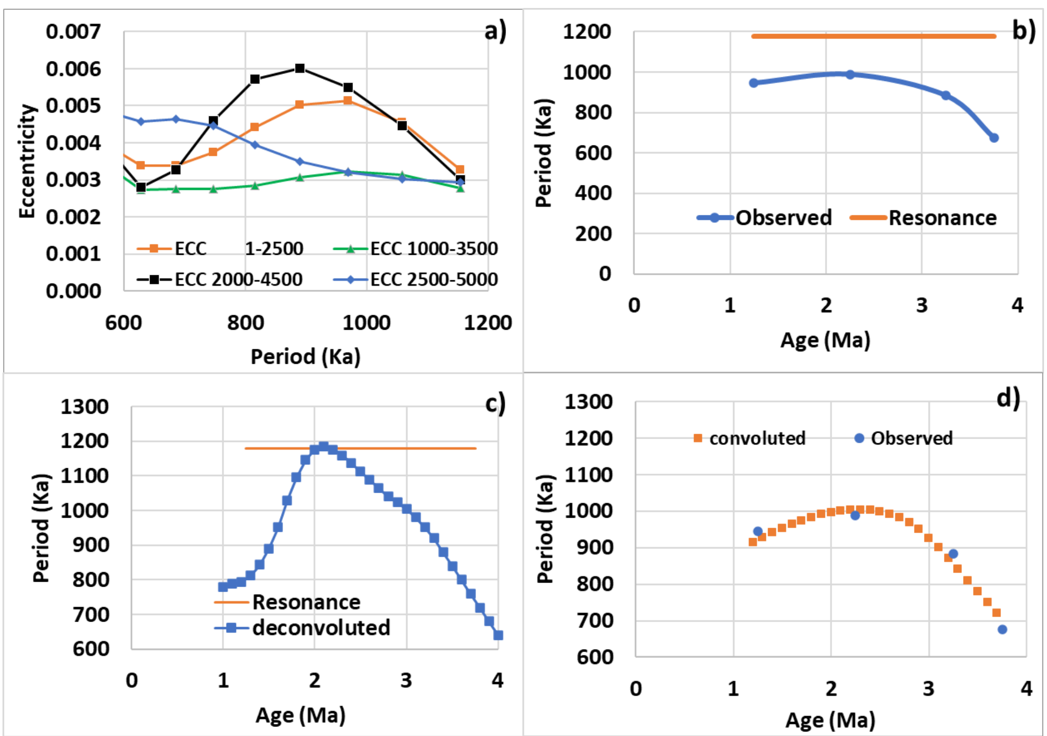

Fig. 5 – Variations in the period of eccentricity in the vicinity of 1000 Ka - a) Fourier transform of eccentricity variations over 2.5 Ma time intervals – b) Periods vs time observed at the maximums of the Fourier transforms in a) – c) Deconvoluted curve of the period vs time represented in b) – d) Comparison of the moving average over 2.5 Ma of the deconvoluted curve in c) and the period vs time in b).

Regarding the 98.3 Ka resonance period, the forcing efficiency has been increasing steadily since 1.4 Ma BP to reach 5 °C (W / m^2) $^{-1}$ at present, which suggests that the tuning continues to improve (Pinault, 2020a) (as explained in Materials and Methods, this efficiency being obtained from EPICA proxies, the value of 4 °C (W / m^2) $^{-1}$ must be considered to be compared with the SST data). The change of the dominant period occurred approximately 1.2 Ma ago.

5 Conclusions

The significance of this research focuses on the high order subharmonic modes of subtropical gyres. While previous work was based on climate archives considered to be representative of the thermal exchanges between subtropical oceanic gyres and the atmosphere, the present research focuses on the direct observation of the South Pacific gyre. All the investigations make it possible to draw up an exhaustive list of subharmonic modes up to n_{15}.

Through this work we have highlighted several unprecedented climatic phenomena that have occurred over the past 3.5 million years. A transition like the MPT occurred about 2.5 million years ago, involving much longer periods. This new approach endows the climate system the aptitude to preferentially respond to certain orbital variations, which is inherited from the resonant forcing of Rossby waves wrapping around the subtropical gyres.

New perspectives have been explored:

1) The poleward drift of the subtropical front of 4° during the MPT highlights an adjustment of the gyre to tune to the forcing period (∼41 Ka) before the MPT while the subharmonic mode n_{10} was dominant. After the MPT the subharmonic mode n_{11} becomes dominant while its natural period approaches the forcing period (∼100 Ka). An increase in the circumference of the gyre of almost 20% without displacement of the centroid allows the subharmonic mode n_{11} to be tuned to the new forcing period while the natural period that characterizes the subharmonic mode n_{10} is regained.
2) Thanks to the high resolution of the climate archive which spans 3.5 million years, the alkenone concentration at DSDP Site 593 presently situated north of the subtropical front allows to extend subharmonic modes beyond n_{11} up to n_{15} (Table 1). It is shown that modes n_{13} and n_{14} are forced because of eccentricity variations while modes n_{12} and n_{15} are pure subharmonics.
3) A transition of the dominant mode between two successive subharmonic modes occurs at the Pliocene-Pleistocene hinge. Like what happens during the MPT, the two subharmonic modes are forced simultaneously, and the natural period of the highest mode optimally tunes to the forcing period when both become very close.

Those new concepts will probably take time to be largely accepted by the scientific community because of their novelty, which requires audacity. The notion of subharmonic modes indeed deeply changes understanding of the paleoclimate, including climate variations observed during the last two centuries (Pinault, 2020b).

Acknowledgments

This study received no funding. The author declares no conflict of interest. Data is available through Berger and Loutre, 1991 and McClymont et al., 2016.

References

Benzi R., Parisi G., Sutera A. & Vulpiani A., (1982) Stochastic resonance in climatic change, *Tellus*, 34:1, 10-15 DOI: 10.3402/tellusa.v34i1.10782

Berger A. & Loutre M.F.. (1991) Insolation values for the climate of the last 10 million years. *Quaternary Science Reviews*, 10, 297-317

Brovkin V.,Calov R., Ganopolski A., Willeit M.. (2019) Mid-Pleistocene transition in glacial cycles explained by declining CO2 and regolith removal | Science Advances. *Science Advances*. 5 (4) doi:10.1126/sciadv.aav7337

Chalk T., Hain M., Foster G., Rohling E., Sexton P., Badger M., Cherry S., Hasenfratz A., Haug G., Jaccard S., Martínez-García A., Pälike H., Pancost R., Wilson P., (2017) Causes of ice age intensification across the Mid-Pleistocene Transition. *Proceedings of the National Academy of Sciences*. 114 201702143. 10.1073/pnas.1702143114

Clark P. U., Archer D., Pollard D., Blum J. D., Rial J. A., Brovkin V., Mix A. C., Pisias N. G., Roy M., (2006) The middle Pleistocene transition: characteristics, mechanisms, and implications for long-term changes in atmospheric pCO2. *Quaternary Science Reviews*. Elsevier. 25 (23–24): 3150–3184 doi:10.1016/j.quascirev.2006.07.008.

Frankignoul C. & Hasselmann K. (1977) Stochastic climate models, Part II Application to sea-surface temperature anomalies and thermocline variability, *Tellus*, 29:4, 289-305 DOI: 10.3402/tellusa.v29i4.11362

Ganopolski A. & Rahmstorf S., (2002) Abrupt Glacial Climate Changes due to Stochastic Resonance, *Phys. Rev. Lett*. 88, 038501

Hasselmann K., (1976) Stochastic climate models Part I. Theory, *Tellus*, 28:6, 473-485 DOI: 10.3402/tellusa.v28i6.11316

Matteucci G., (1991) A study of the climatic regimes of the Pleistocene using a stochastic resonance model. *Climate Dynamics* 6, 67–81 https://doi.org/10.1007/BF00209981

McClymont E. L., Elmore A. C., Kender S., Leng M. J., Greaves M., & Elderfield H. (2016) Pliocene-Pleistocene evolution of sea surface and intermediate water temperatures from the southwest Pacific, *Paleoceanography*, 31, 895–913 doi:10.1002/2016PA002954

Nicolis C. (1982) Stochastic aspects of climatic transitions–response to a periodic forcing, *Tellus*, 34:1, 1-9 DOI: 10.3402/tellusa.v34i1.10781

Pinault J-L, (2018a) Resonantly Forced Baroclinic Waves in the Oceans: Subharmonic Modes, *J. Mar. Sci. Eng.*, 6, 78; doi:10.3390/jmse6030078

Pinault J-L, (2018b) Modulated Response of Subtropical Gyres: Positive Feedback Loop, Subharmonic Modes, Resonant Solar and Orbital Forcing, *J. Mar. Sci. Eng.*, 6, 107; doi.org/10.3390/jmse6030107

Pinault J-L, (2018c) Anthropogenic and Natural Radiative Forcing: Positive Feedbacks, *J. Mar. Sci. Eng.*, 6, 146; doi:10.3390/jmse6040146

Pinault J-L, (2020a) Resonant Forcing of the Climate System in Subharmonic Modes, *J. Mar. Sci. Eng.*, 8, 60; doi:10.3390/jmse8010060

Pinault J-L, (2020b) The Moist Adiabat, Key of the Climate Response to Anthropogenic Forcing, *Climate*, 8, 45 doi:10.3390/cli8030045

Saravanan R., & McWilliams J. C., (1997) Stochasticity and Spatial Resonance in Interdecadal Climate Fluctuations, *J. Climate* 10 (9): 2299–2320 https://doi.org/10.1175/1520-0442(1997)010<2299:SASRII>2.0.CO;2

Timmermann A., Gildor H., Schulz M., Tziperman E., (2003) Coherent Resonant Millennial-Scale Climate Oscillations Triggered by Massive Meltwater Pulses, *Journal of Climate*, 1

Torrence C. & Compo G.P., (1998) A practical guide for wavelet analysis. *Bull. Am. Meteorol. Soc.*, 79, 61–78

Ya S. V., (1980) Origin and mechanism of large-scale climatic oscillations. *Science* 209:1477–1482